European Journal of Pharmaceutical Sciences 111 (2018) 73–82

Contents lists available at ScienceDirect

European Journal of Pharmaceutical Sciences

journal homepage: www.elsevier.com/locate/ejps

Mucoadhesive nanostructured polyelectrolytes complexes modulate the intestinal permeability of methotrexate

Fernanda Isadora Boni[a], Andreia Almeida[b,c], Anna Lechanteur[c,e], Bruno Sarmento[b,c,d,*], Beatriz Stringhetti Ferreira Cury[a], Maria Palmira Daflon Gremião[a]

[a] UNESP - São Paulo State University, School of Pharmaceutical Sciences, Rod. Araraquara-Jaú, Km 01, CEP: 14801-902 Araraquara, Brazil
[b] i3S - Instituto de Investigação e Inovação em Saúde, Universidade do Porto, Rua Alfredo Allen, 208, 4200-135 Porto, Portugal
[c] INEB - Instituto de Engenharia Biomédica, Universidade do Porto, Rua Alfredo Allen, 208, 4200-135 Porto, Portugal
[d] CESPU - Instituto de Investigação e Formação Avançada em Ciências e Tecnologias da Saúde, Rua Central de Gandra 1317, 4585-116 Gandra, Portugal
[e] Laboratory of Pharmaceutical Technology and Biopharmacy, CIRM, Universite of Liège, Liège 4000, Belgium

ARTICLE INFO

Keywords:
Intestinal permeability
Caco-2 monoculture
Triple co-culture cell model
Chitosan
Polyelectrolytes complexes
Mucoadhesive
Methotrexate

ABSTRACT

Nanostructured polyelectrolytes complexes (nano PECs) loaded with methotrexate (MTX) were obtained by the polyelectrolyte complexation of chitosan (CS) and hyaluronic acid (HA), further incorporating hypromellose phthalate (HP). The mean diameter of nano PECs ranged from 325 to 458 nm, with a narrow size distribution. Zeta potential was close to + 30 mV, decreasing to + 21 mV after the incorporation of HP, a range of values that favour the physical stability of system as the interaction with cationic biological membranes. The electrostatic interactions between the different components were indicated by the FTIR data. The mucoadhesiveness of nano PECs was demonstrated and MTX and HP influenced this property. The cell viability assays showed the biosafety of the isolated polymers and nano PECs in intestinal HT29-MTX and Caco-2 cell lines at 4 h of test. The permeability values of MTX loaded in CS/HA nano PECs were 7.6 and 4-fold higher than those of CS/HA/HP nano PECS and free drug, respectively, in the Caco-2 monoculture. In mucus secreting co-culture cell model these values were 3 and 6.5 fold, respectively. Such features indicate that nano PECs developed in this work can be promising carriers for MTX in the treatment of local or systemic diseases.

1. Introduction

Methotrexate (MTX) is an antifolate cytotoxic drug, in higher doses is currently used in the treatment of several solid tumours such as those in colorectal and, in lower doses MTX has shown a promise activity as an immunomodulatory drug, being used successfully in the treatment of systemic inflammatory diseases (Gaies et al., 2012; Higano and Livingston, 1989; Jachens and Chu, 2008; Jain et al., 1979; Martins and Yamamoto, 2008). Several dosing regimens can be adopted in MTX therapy, by oral route, for the treatment of such diseases (Gorlick et al., 1997; Widemann and Adamson, 2006). MTX is classified as class III in the Biopharmaceutical Classification System (high solubility and low permeability), a limiting property when the therapy requires the systemic absorption. Another issue is the low oral bioavailability of MTX due to the action of the P-glycoprotein (P-gp) as an efflux pump (Barrueco et al., 1992; Borst et al., 1999; Huber et al., 2010). To overcome these problems, an excess of drug is usually administered but the side effects are thus exacerbated (Barrueco et al., 1992; Thiebaut et al., 1987).

The pharmaceutical nanotechnology is a relevant technological tool that enables the building of new nanostructures with different and improved properties, allowing the protection of drug against premature degradation by the gastrointestinal tract (GIT) enzymes or low pH value of gastric fluid and the modulation of the drug release rates or the targeting of drug for specific organs or tissues (Hamidi et al., 2008; Janes et al., 2001). Nanostructured polyelectrolytes complexes (nano PECs) are obtained by the polyelectrolyte complexation technique; which adds important technological advantages as the simplicity of execution and relative low cost process. An important property of the nano PECs intended to the oral route of administration is the mucoadhesiveness. This property may prolong the nano PEC residence time at the absorption site, promoting a closer contact with the epithelial barrier, favouring the local interaction with the site of action or the systemic absorption. The mucoadhesive property of natural polymers as chitosan (CS), hypromellose phthalate (HP) and hyaluronic acid (HA), in the GIT, have been explored in the design of nano PECs (Ensign et al., 2012; Pedreiro et al., 2016). CS is a biocompatible and biodegradable cationic polysaccharide; due to the deprotonation of their

* Corresponding author at: Instituto de Investigação e Inovação em Saúde, Universidade do Porto, Rua Alfredo Allen, 208, 4200-135 Porto, Portugal.
E-mail address: bruno.sarmento@ineb.up.pt (B. Sarmento).

http://dx.doi.org/10.1016/j.ejps.2017.09.042
Received 26 June 2017; Received in revised form 11 September 2017; Accepted 26 September 2017
Available online 28 September 2017
0928-0987/

amino groups, composed by D-glucosamine and *N*-acetyl-D-glucosamine units linked by β-1,4 linkages (Rinaudo, 2011; Wang et al., 2012). The ability of CS to open the cellular tight junctions improving the drug permeability has been extensively reported (Sarmento et al., 2007; Vllasaliu et al., 2010; Wang et al., 2017). For oral route, the high solubility of CS in acidic pH is a drawback, so that the association with HP, an enteric coating polymer, could be a rational way to prevent the drug premature release. Besides, HP is able to form polyelectrolytes complexes with cationic polyelectrolytes (Meehan, 2006). The HA is an anionic polysaccharide, biocompatible and biodegradable with high molecular weight, composed by D-glucuronic acid and *N*-acetyl-D-glucosamine. HA is an important component of many tissues and extracellular matrix and has the ability to interact specifically with CD44 receptors, expressed in the surface of intestinal epithelial cells, responsible for the transmission of internalization signals (Becker et al., 2009; Liao et al., 2005; Ponta et al., 2003). Thus, the incorporation of HA into the nano PECs could contribute to the mucoadhesiveness, improving the biological interaction of the system.

In this work CS/HA nano PECs with or without HP, loaded with MTX, were obtained and characterized by physical-chemical properties and drug association efficiency. The biological interaction of the systems was evaluated by mucoadhesiveness and intestinal *in vitro* permeability assays; using monoculture model of Caco-2 cells and mucus producing triple co-culture model of Caco-2:HT29-MTX:Raji B cells.

2. Materials and methods

2.1. Materials

2.1.1. Chemical materials

Low molecular weight chitosan (Mw ≈ 200 kDa; deacetylation degree of 90%) was obtained from Sigma Aldrich® (St. Louis, MO, USA). Hypromellose phthalate (phytalyl content of 31%) from Shin-Etsu® (Tokyo, Japan). High molecular weight sodium hyaluronate (Mw ≈ 1000 kDa; glucuronic acid content of 47%) was obtained from ViaFarma (São Paulo, Brazil) and methotrexate from Fagron (São Paulo, Brazil). All the other materials used were of analytical grade and obtained from commercial suppliers.

2.1.2. Cell line and culture

C2BBe1 clone of Caco-2 was obtained from American Type Culture Collection (ATCC, USA), HT29-MTX and Raji B were provided by Dr. T. Lesuffleur (INSERMU178, Villejuif, France) and by Dr. Alexandre Carmo (Cellular and Molecular Biology Institute – IBMC, Porto, Portugal), respectively. The cells were cultured with Dulbecco's modified Eagle medium (DMEM) from Lonza (Verviers, Belgium), supplemented with 10% (v/v) Fetal Bovine Serum (FBS), 1% (v/v) penicillin (100 U/mL) and streptomycin (100 µg/mL), 1% (v/v) non-essential amino acids (NEAA). All these supplements were purchased from Invitrogen Corporation (Life Technologies, S.A., Madrid, Spain). The reagents 3-(4,5-Dimethylthiazol-2-yl)-2,5-diphenyltetrazolium bromide (MTT), 4′,6-diamidine-2′-phenylindole dihydrochloride (DAPI) and dimethyl sulfoxide (DMSO) were obtained from Sigma Aldrich® (St. Louis, MO, USA) and Triton X-100 from Spi-Chem (West Chester, PA, USA). Paraformaldehyde (PFA) was purchased from Merck Millipore (Billerica, MA, USA), Alexa Fluor® 546 Phalloidin and Goat anti-rabbit Alexa-Fluor 488® secondary antibodies was purchased from Molecular Probes® (Life Technologies S.A., Madrid, Spain). Rabbit occludin primary antibody was obtained from Santa Cruz Biotechnology (Heidelberg, Germany). Fluorescence mounting medium was purchased from Dako (Peterborough, UK). The culture flasks and 96-well tissue culture plates were purchased from Corning Inc., (Steuben County, NY, USA) and the 6-wells plates Transwell™ (PET membrane, pore size of 3 µm) was obtained from Corning, Madrid, Spain. The cells were maintained in a conventional incubator (Binder® CB 210, Germany) at 37 °C and 5% CO_2 in a water-saturated atmosphere.

2.2. Determination of molecular weight of polymers

The molecular weight (*Mw*) and second virial coefficient (A_2) of CS, HA and HP were estimated by the static light scattering technic on a Zetasizer Nano ZS® (Malvern Instruments, Worcestershire, UK) equipment, using the Zetasizer nano ZS v7.11 software (Worcestershire, UK). Polymers dispersions, in different concentrations (0.02–0.9 mg·mL^{-1}) at 25 °C were analysed implementing the Rayleigh equation, that describes the intensity of light scattered from the polymer structure in solution (Ferreira et al., 2017). The experiment was conducted using toluene, previously filtered through a polytetrafluoroethylene membrane (PTFE, 0.2 µm), as an equipment internal standard and ultra-pure water filtered through a cellulose acetate membrane (RC, 0.2 µm), as the blank. CS, HA and HP were dispersed in filtered acetic acid (0.1 M), ultra-pure water and sodium hydroxide (0.1 M), respectively. Applied refractive index increments (dn/dc) were 0.181 mL·g^{-1} for the CS, 0.152 mL·g^{-1} for the HP and 0.167 mL·g^{-1} for the HA (Fukasawa and Obara, 2003; Hokputsaa et al., 2003; Schatz et al., 2003). For each concentration, the scattering intensity was measured, in triplicate.

2.3. Preparation of nanostructured polyelectrolytes complexes

Nano PECs composed by CS/HA and CS/HA/HP were obtained by the polyelectrolyte complexation technic (Makhlof et al., 2011; Pedreiro et al., 2016). CS was first dispersed overnight in acetic acid 0.1 M (0.5 mg/mL) and added slowly in an aqueous dispersion of HA (0.1 mg/mL), under magnetic stirring for 15 min (1:0.2, w/w). Afterwards, for the samples with HP, the polymer dispersed in sodium hydroxide 0.1 M (0.5 mg/mL) was added to the preformed particles (1.0:0.2:0.2, w/w/w), under magnetic stirring for 30 min. Before the complexation process, the pH values of all polymers dispersions were adjusted to 5.5. Drug loaded nano PECs were prepared by the previously MTX solubilisation in sodium hydroxide 0.1 M (2.0 mg/mL) and it addition into the CS dispersion, to the final concentration of 5% (w/w). Nano PECs were labelled according to the polymeric content as NpHA for CS/HA in the composition and NpHP for CS/HA/HP in the composition. The suffixes -MTX and -0 and were used for samples containing or not drug, respectively.

2.4. Characterization of nanostructured polyelectrolytes complexes

The average hydrodynamic diameter and zeta potential (ZP) analyses of NpHA-0, NpHP-0, NpHA-MTX and NpHP-MTX were performed by the dynamic light scattering technic (DLS) and electrophoretic light scattering, at 25 °C, in a detection angle of 173° using the equipment Zetasizer Nano ZS®. Analyses were performed in triplicate and the results were expressed by the average of 10 determined values and its standard deviation. The nano PECs morphology was also analysed by field emission gun scanning electron microscopy (FEG-SEM; JEOL JSM-7500F, Japan). Samples were diluted (1:30, v/v), placed on a metallic holder and dried at room temperature (RT). After, samples were covered with carbon and photomicrographs at different magnification were taken. In order to evaluate polymer-polymer and polymer-drug interactions, the FTIR (Fourier transform infrared spectroscopy) of isolated polymers, free MTX and nano PECs were recorded at RT with a VERTEX 70 spectrometer BRUKER (Massachusetts, USA) and ATR accessory, by the attenuated total reflection method (diamond crystal). For each sample, 64 scans were recorded between 3600 and 400 cm^{-1}.

To determine the %AE, a known volume of the NpHA-MTX and NpHP-MTX dispersions were centrifuged at 14,000 rpm in an ultracentrifuge (ThermoScientific, Massachusetts, USA), for 30 min. The supernatant was filtered through a cellulose acetate membrane (0.20 µm) and analysed by spectrophotometry in a multimode plate reader (Biotek Synergy 2, Winooski, VT, USA) at 303 nm. Tests were performed in triplicate, and the %AE was calculated according the Eq. (1).

$$\%AE = \frac{(AA - FA)}{AA} \times 100 \quad (1)$$

where AA was the total amount of drug added, and FA was the quantified amount of free drug in the supernatant.

2.5. Assessment of mucoadhesion of nanostructured polyelectrolytes complexes

Tensile strength measurements were performed in a TA-XTplus texture analyser (Stable Micro Systems, Surrey, UK) using porcine intestine as a mucosal model. The intestine was carefully cleaned, cut in pieces with 4 cm^2, hydrated with phosphate buffer pH 6.8 at 37 °C and fastened to the equipment platform. The nano PECs were previously frozen in an Ultra low Freezer (Sanyo, MDF-U76VC, Japan), at − 80 °C and, lyophilized during 48 h (Micro Modulyo 115, Thermo Scientific, Waltham, USA). Nano PECs and polymers were fixed to the upper movable cylindrical probe (10 mm of diameter), using double side adhesive tape. The measurement was triggered to begin as the upper probe encountered the resistance force of the mucosal tissue, the contact was kept for 120 s, with no force applied. After 120 s, the probe was raised at a constant speed of 0.5 mm/s and the force (Fm, N) needed for sample and intestinal mucosa detachment were registered (Carvalho et al., 2013; Varum et al., 2010).

2.6. Cellular assays

2.6.1. Cell viability studies

Cell viability experiments were performed on Caco-2 and HT29-MTX colorectal cells lines, using the MTT reagent. Both cells lines were cultivated separately in culture flasks, with complete medium with the composition described in Section 2.1. Caco-2 and HT29-MTX were seeded into 96-well plates at density of 2×10^4 cells/well and 1×10^4 cells/well, respectively, and incubated at 37 °C in 5% CO_2 atmosphere for 24 h, to allow the attachment to the wells. On the next day, the wells medium was removed and cells were washed once with phosphate buffered saline (PBS) following with 4 h and 24 h of incubation with free MTX, polymers, empty and loaded nano PECs in the concentration range of 0.01 to 100 μg/mL. The background was DMEM, the positive and negative controls were cells incubated with DMEM and Triton X-100 1% (w/v), respectively. After the incubation time, the tested samples were removed and cells were washed with PBS. The MTT solution (0.5 mg/mL) was added followed by the incubation for 2–3 h in the dark. Subsequently, the MTT solution was removed and DMSO was added to dissolve the formed formazan crystals, under shaking for 30 min in the dark. The absorbance was measured using a multimode plate reader (Biotek Synergy 2, Winooski, VT, USA) at 570 and 630 nm (Almeida et al., 2017; Silva et al., 2017). The viability percentage was calculated according the Eq. (2).

$$Cell\ viability\,(\%) = \frac{experimental\ value - negative\ control}{positive\ control - negative\ control} \times 100 \quad (2)$$

2.6.2. In vitro intestinal permeability studies

The experiment was performed according to the previously reported work of Antunes et al. (2013) and Araujo and Sarmento, 2013in a monoculture model of Caco-2 cells and triple co-culture model; consisted in Caco-2:HT29-MTX:Raji B. The models were seeded in a 6-well Transwell™ plates (transparent PET membrane, 3 μm pore diameter, 4.67 cm^2). Caco-2 and Caco-2:HT29-MTX cells were seeded on the apical chamber of the Transwell™ insert and maintained in the same culture conditions for 14 days, with medium changes every other day. After that time, Raji B cells were added to the basolateral compartment of Caco-2:HT29-MTX wells, to complete the triple model formation. Both models were maintained for more 6–7 days, until forming a monolayer (Antunes et al., 2013; Araujo and Sarmento, 2013).

First, to perform the permeability experiment, the medium of the apical and basolateral sides of the Transwell™ was removed and cells were washed twice with prewarmed HBSS. Then, both sides of the Transwell™ were filled with fresh HBSS and allowed to equilibrate for 30 min, at 37 °C, in an orbital shaking incubator (IKA® KS 4000 IC) at 100 rpm. Permeability studies of free MTX, NpHA-MTX and NpHP-MTX dispersions at concentration 100 μg/mL, were performed in triplicate during 4 h. At predetermined time intervals (5, 15, 30, 45, 60, 120, 180 and 240 min), aliquots of 200 μL were withdrawn from the basolateral chamber of the insert and immediately replaced with fresh HBSS. At the end of the experiment, an aliquot of the apical compartment medium was removed for the drug quantification (Almeida et al., 2017; Silva et al., 2017). After, the inserts were washed twice with HBSS and incubated for 30 min, at 37 °C, to the layer equilibrium. Subsequently, cells were detached from the insert using 200 μL of trypsin and lysed with 1.5 mL of Triton-X overnight and then, centrifuged at 14,000 rpm for 20 min to the cells fragments separation. The supernatants were removed and filtrated to quantify the amount of MTX bounded or within the mucus layer or cell monolayer (Shrestha et al., 2016). All experiments were performed in triplicate, for each sample, and the MTX was quantified by UV–Vis spectrophotometer (Biotek Synergy 2, Winooski, VT, USA), at 303 nm.

The cells monolayer integrity was evaluated before, during and at the end of permeability experiment by measuring the transepithelial electric resistance (TEER) using an EVOM Epithelial Volthometer Instrument equipped with a chopstick electrode (World Precision Instruments, Sarasota, FL, USA).

The results were expressed in percentage of permeability and drug apparent permeability (Papp) that was calculated using the Eq. (3).

$$Papp = \frac{\Delta Q}{A \times C_0 \times \Delta t} \quad (3)$$

where ΔQ is the amount of drug quantified in the basolateral side (μg), A is the surface area of the insert (cm^2), C_0 is the initial drug concentration in the apical side of the Transwell™ (μg/mL) and Δt is the experiment duration (seconds).

2.6.2.1. Confocal laser scanning microscopy. The confluence and integrity of monolayers were analysed with confocal microscopy after the permeability assay. Cells on Transwell™ were fixed with 2% (w/v) paraformaldehyde (PFA) for 30 min and permeabilized by incubating for 7 min with 0.2% (v/v) Triton X-100 in PBS. The blocking was done with PBST (PBS (1 ×) containing 0.05% (v/v) Tween-20) containing 10% (v/v) in 10% (v/v) FBS for 30 min. Tight junctions were stained with a rabbit occludin primary antibody (1:50) during 2 h at RT, following with goat anti-rabbit Alexa-Fluor 488 secondary antibody (1:200) during 1 h at RT, both diluted in PBST containing 5% (v/v) FBS. Cell nucleus was counterstained with DAPI (1:1000). The membrane was washed three times with PBS, cut and mounted on a glass slide with fluorescence mounting medium.

2.7. Statistical analyses

The experimental results are represented as mean ± standard deviation (SD). One-way analysis of variance (ANOVA) followed by Tukey's test at significance level of 5% was used to compare different groups using GraphPad Prism® software (Prism 6 for Windows, CA, USA).

3. Results and discussion

3.1. Molecular weight of polymers

Molecular weight (*Mw*) and second virial coefficient (A_2) are important parameters that can be manipulated and evaluated to engineering nanoparticulated systems with better process yield and

Table 1
Polymers molecular weight (*MW*) and second virial coefficient (A_2).

Polymer	*Mw* (kDa)	A_2 (mL·mol/g^2)
CS	106.38 ± 3.78	$0.002435 \pm 9.12.10^{-5}$
HA	1294.06 ± 41.94	$0.0136 \pm 9.9.10^{-4}$
HP	75.18 ± 3.99	$0.0702 \pm 8.51.10^{-3}$

desired characteristics. The values of Mw and A2 are shown in Table 1.

CS *Mw* could vary by source of extraction and obtainment process. The commercially available CS *Mw* are comprised between 50 and 2000 kDa, in this study the CS used to nano PECs development presented a low *Mw* (Meera and Abraham, 2006; Rinaudo, 2011). Low molecular weight CS has promising characteristics for drug delivery systems development as higher biodegradability and biocompatibility, compared to the high *Mw* CS (Chae et al., 2005) and it can allow to the formation of smaller and spherical particles (Gao et al., 2005; Yang et al., 2014). For the HP, a high *Mw* was observed (Table 1). This kind of cellulose derivative has a greater resistance to the acidic pH and, consequently, it is more efficient in the design of systems that the aim is to control drug release rates in the upper portions of the gastrointestinal tract (Meehan, 2006; Wang et al., 2004). The HA analysed presented a high (Table 1), this glycosaminoglycan is able to interact specifically with cellular membrane receptor and could be constituted of up to 10,000 disaccharides, characteristic that gives a bulky and rigid structure to the molecule. This type of HA is biodegradable, non-immunogenic and has a potential anti-angiogenic action, unlike to low *Mw* HA; which signalling important inflammatory, metastatic and immunogenic events (Mizrahy et al., 2011). The A_2 is an important parameter that describes the interaction force between the polymer and the solvent. Positive A_2 values indicate a strong polymer-solvent interaction, which means that the chosen solvent is suitable for the solvation of polymer chains. In case of strong intra/intermolecular polymer interaction, the A_2 value will be negative and, consequently, the chosen solvent contribute to the molecular agglomeration (Murphy, 1997). For CS, HP and HA, the A_2 values were positive (Table 1), thus, the chosen solvents for the polymer dispersion were appropriated to the subsequent use in nano PECs obtainment. Since the solvents should minimize the intra/intermolecular aggregation, making the CS amine groups and HA/HP carboxyl groups more available for the electrostatic interaction and nano PECs formation (Valente et al., 2005).

3.2. Characterization of nanostructured polyelectrolytes complexes

The nano PECs were spontaneously formed at pH value of 5.5, by the mixture of the polyelectrolytes with opposite charges (positive charged CS and negative charged HA and HP). Based on the polyelectrolytes complexes development theory, during the nano PECs formation, it was believed that the ionized high molecular weight HA was able to attract the CS molecules, primarily by electrostatic forces, accommodating them in their structure. Consequently, additional hydrogen bonds were formed resulting in a structural rearrangement of the polymers chains. For samples with HP, it is possible that the polymer molecules were deposited around and inside the CS/HA preformed matrix (Schatz et al., 2004).

The average diameter of NpHA-0 and NpHP-0 were 426.4 nm and 450.5 nm, respectively (Table 2), shown that the HP addition had not significant effect on the size of nanoparticles. The PdI values of NpHA-0 and NpHP-0 were around 0.28 and 0.26, respectively, indicating the homogeneity of particles size (Gaumet et al., 2008). NpHA-0 exhibited high positive average ZP value (+ 33.1 mV). For sample NpHP-0, the addition of HP reduced significantly this value to + 26.0 mV (Table 2).

For the samples NpHA-MTX and NpHP-MTX, an average diameter of 447.2 nm and 325.7 nm, respectively, was observed (Table 2), demonstrating that the drug loading reduced the diameter by around 124 nm, for the sample containing HP. MTX, at the pH value of polymer dispersion (5.5), is negatively charged thus we can suggest that the drug promoted additional points of electrostatic interaction between the ionizable groups of the CS, resulting in the packaging of the polymer network and, consequently, in smaller particle (Abolmaali et al., 2013).

The PdI values observed for the samples with MTX were 0.24 and 0.28, indicating homogeneity of the size. A significant reduction on ZP values after the MTX addition, compared to the samples without drug, was observed (Table 2). However, even after the drug addition, ZP values were positive, ranging from + 20.9 to + 29.6 mV.

The positive surface charges of nanoparticles can favour the adhesion to the anionic mucus layer of intestine, prolonging the residence time in the target site and making closer the contact with biological membrane (Asane et al., 2008; Boni et al., 2016; Gamboa and Leong, 2013). After the nanocarriers mucoadhesion, whether the accumulation in target cells or the permeation through the intestinal membrane will be the prevalent process is what will determine the extension of local or systemic action.

The nano PECs %AE ranged from 30.0 to 37.4%, for NpHA-MTX and NpHP-MTX, respectively, being observed a greater association of MTX for the nanoparticle with HP. These values are higher than those found by Cascone et al. (2002) with gelatin nano PECs (5%–15.6% of MTX incorporated) and Trapani et al. (2011) for CS and glycochitosan nano PECs (19–48% of MTX association) (Cascone et al., 2002; Trapani et al., 2011).

SEM photomicrographs confirmed the nanometric scale of particles and their spherical shape (Fig. 1). As it is possible to observe, the MTX addition did not change the spherical shape of nano PECs. However, for NpHP-MTX the presence of a wide range of size and higher degree of agglomeration, compared to those without drug was observed (Fig. 1), possibly due to the higher association of the drug (Table 2) into the matrix and the reduction of the ZP; which consequently reduced the electric repulsion between the nano PECs.

FTIR analysis was performed in order to identify any indicative of chemical interaction due to the polyelectrolyte complexation process. The Fig. 2(A) shown the characteristic absorption bands of the polymers (Haxaire et al., 2003; Li et al., 2013; Pedreiro et al., 2016; Reddy and Karunakaran, 2013) and MTX (Chadha et al., 2009; Zhang et al., 2012). In the MTX spectra, was identified two broad bands between 3400 and 3150 cm^{-1} related to the N—H stretch of the aliphatic primary amine and to the hydroxyl (OH) of the molecule carboxylic acid. At approximately 1650 cm^{-1} was observed the absorption band of C=C stretch of the aromatic ring and at 1608 cm^{-1}, the absorption referring to the amide N—H vibration. In the region of 1641 cm^{-1} there was an absorption band of the C=O bond, at 1240 cm^{-1} attributed to the

Table 2
Values of diameter (nm), particle size distribution (PdI) and association efficiency (%AE) of nano PECs.

Sample	Average diameter (nm) ± SD	PdI	Average zeta potential (mV) ± SD	%AE ± SD
NpHA-0	$426.4 \pm 12.3^{a,b}$	0.26^{a}	$+33.1 \pm 0.4^{a}$	–
NpHP-0	450.5 ± 69.1^{a}	0.28^{a}	$+26.0 \pm 2.1^{b}$	–
NpHA-MTX	446.9 ± 29.7^{b}	0.24^{a}	$+29.6 \pm 1.5^{c}$	30.0 ± 1.2^{b}
NpHP-MTX	325.7 ± 17.6^{c}	0.28^{a}	$+20.9 \pm 1.4^{d}$	37.4 ± 3.8^{a}

[a, b, c] and [d] denote a significant difference between each sample determined using Tukey's multiple comparison test ($p < 0.05$).

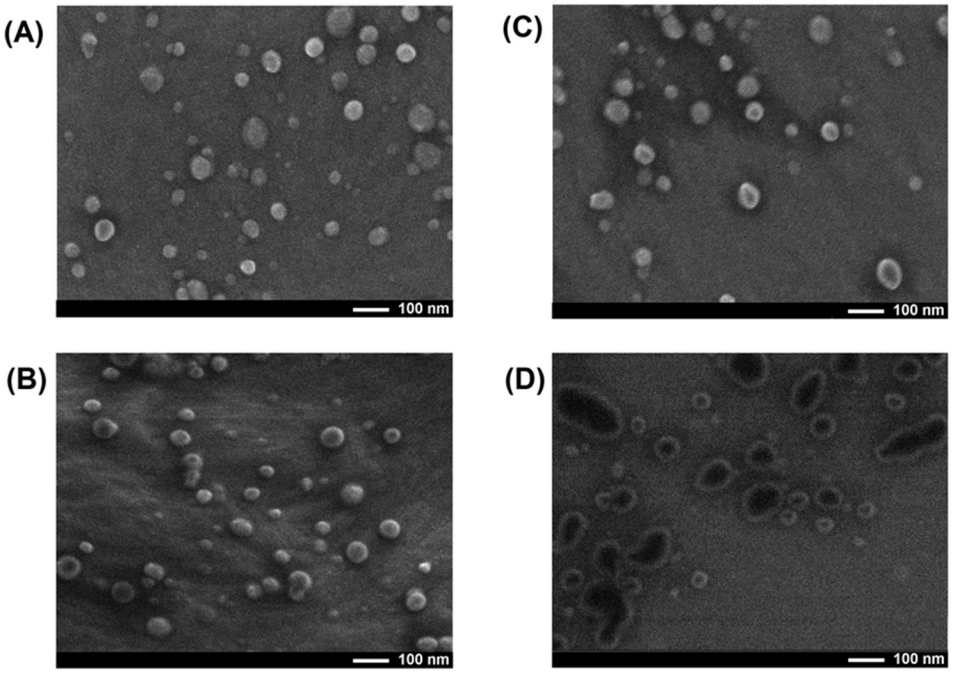

Fig. 1. Photomicrographs of (A) NpHA-0; (B) NpHA-MTX; (C) NpHP-0 and (D) NpHP-MTX (50,000 ×).

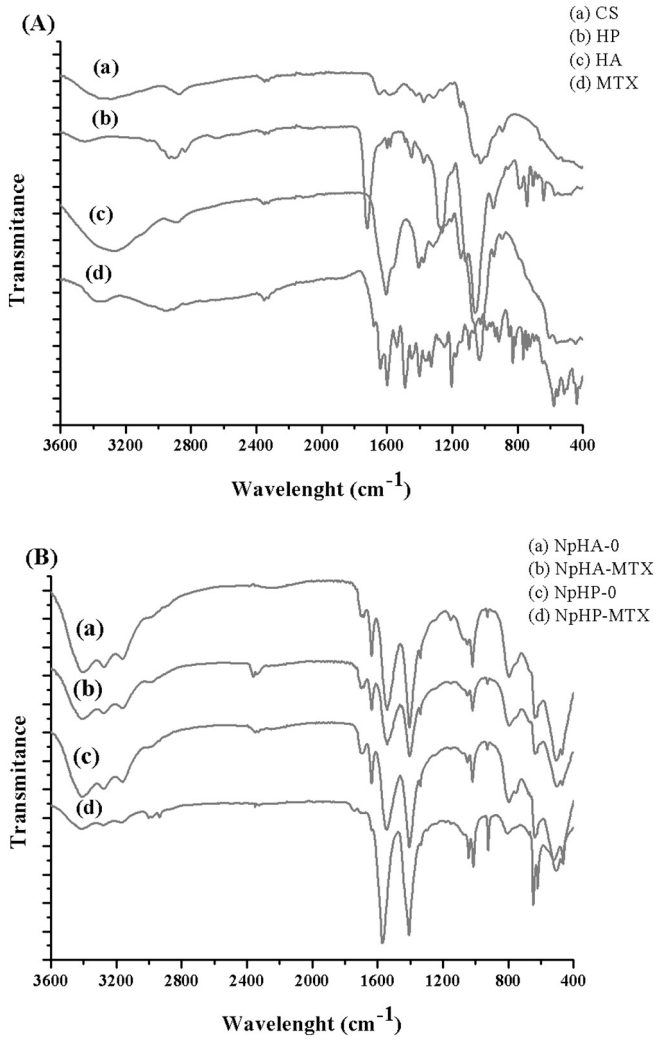

Fig. 2. Fourier transform infrared spectroscopy (FTIR) spectra of (A) Polymers and MTX, (B) NpHA-0, NpHA-MTX, NpHP-0 and NpHP-MTX.

absorption of the CN stretch and at 1470 cm^{-1} corresponding to MTX aromatic rings (Chadha et al., 2009). The HP spectra shows a broad band between 3500 and 3250 cm^{-1} which represents the stretching of the OH group and an absorption, attributed to the sp^3 hybridization CH bond, was also identified at approximately 2800 cm^{-1}. In 1725 cm^{-1} a strong band characteristic of the C═O of the ester function probably overlap the adsorption of C═O stretch of carboxylic acid. Between 1600 and 1500 cm^{-1} a low intensity band of the aromatic ring stretch was identified. At about 1100 cm^{-1} the well-defined band observed corresponding to CO of the ether function and a band at 690 cm^{-1} characteristic of the ortho-disubstituted aromatic ring (Pedreiro et al., 2016). For the HA, the OH stretch band was present between 3500 and 3250 cm^{-1}. At 1625 cm^{-1}, the C═O stretch signal of the carboxylic acid probably overlaps the C═O bond of the secondary amide function which also exhibits the characteristic stretching CN band and NH folding at approximately 1490 cm^{-1}. The observed low intensity band at 1125 cm^{-1} probably refers to the asymmetric C−O−C bond of the glycosidic group and at approximately 1000 cm^{-1} the high intensity absorption can be attributed to the C−O stretch (Haxaire et al., 2003; Reddy and Karunakaran, 2013). In the CS FTIR spectra, it was observed bands between 3500 and 3250 cm^{-1} referring to the stretching of the OH group, in 1680 cm^{-1} the band assigned to (−CO) NH_2 of the CS primary amide, in 1580 cm^{-1} referred to the axial deformation of the NH_2 (Fig. 2(A)) (Li et al., 2013; Pedreiro et al., 2016).

The ionizable groups of CS, HA and HP are involved in the process of complexation and nano PECs formation. In this sense, was tried to evaluate the interference in the materials absorption frequencies, with band displacements and appearance of new bands that could indicate the occurrence of intermolecular interactions. Empty and loaded nano PECs showed characteristic spectra, in which was observed a displacement in the bands of (−CO) NH2 and NH2 groups from CS for 1680 and 1580 cm^{-1} to approximately 1620 and 1530 cm^{-1}, respectively, indicating the possible interaction of CS with the polyanions, in the nano PECs formation (Fig. 2 (B)). As a result of this interaction there was a formation of $+NH_3$, confirmed by the absorption band at approximately 3350 cm^{-1} in Fig. 2 (B). Regarding to the anionic polymers, the formation of intermolecular bonds can be indicated by two bands observed in the 1725 cm^{-1} band, attributed to C═O binding, present in HP and 1490 cm^{-1} characteristic of HA. The significant reduction of the intensity of these bands, compared to the spectra of the

free polymers, is a strong indication of the process of complexation and formation of hydrogen bonds indicated by the appearance of the band at approximately 1050 cm^{-1} (Sarmento et al., 2007). For samples containing MTX, an increase in band intensity was observed at 3350 cm^{-1}; may indicate the formation of + NH3, from the interaction between the drug and the CS. Overlapping this band, was the band referring to the aliphatic primary amine of MTX. It was also observed a higher intensity of the band between 1490 and 1470 cm^{-1}, possibly as a result of the overlap of the absorption of the MTX aromatic rings and C═O bond of the HA in the structure, and of the band at 1050 cm^{-1} as a result of the formation of greater number of hydrogen bonds between drug and polymers (Fig. 2(B)).

3.3. Mucoadhesion of nanostructured polyelectrolytes complexes

The intestinal epithelia are covered by a layer of mucus, responsible for the GIT protection and lubrication (Varum et al., 2008). The mucus layer that covers the mucosal tissue presents a complex structure; which also differs in concentration of mucin, thickness and pH, around the GIT. All these factors should be considered, since they directly influence in the mucoadhesion process (Madsen et al., 1998; Sosnik et al., 2014). This *ex vivo* assay aimed to mimic the intestinal conditions in which the system will be exposed. The mucoadhesive test was performed with the polymers CS, HA and HP individually and with each formulation of NpHA-0, NpHA-MTX, NpHP-0 and NpHP-MTX. The contact stage, involved in the mucoadhesion process, was imposed using the mechanical energy of the equipment and the strength required to separate the substrates, after the consolidation stage, was evaluated.

For the CS the Fm was 0.444 N while for the polymers HA and HP the values were lower, around 0.180 N, as shown in Fig. 3. The CS is a polycation and presents the capacity to establish electrostatic interaction with the mucin, besides is able to form hydrogen and hydrophobic connections, making this material important in the development of mucoadhesive systems (Sosnik et al., 2014). In contrast, HA and HP, both anionic polymers, presented lower Fm (Fig. 3), but both are also capable of promoting mucoadhesion because there hydrophilicity, by the presence of non-covalent secondary linkages, such as hydrogen and flexible chains, that can favour the interpenetration in the mucus layer, according to the diffusion theory (Andrews et al., 2009; Carvalho et al., 2010).

Between the samples without drug, it is possible to observe, that the presence of HP did not significantly influenced the mucoadhesion force (Fm) ($p > 0.05$), but the MTX addition significantly decrease the Fm

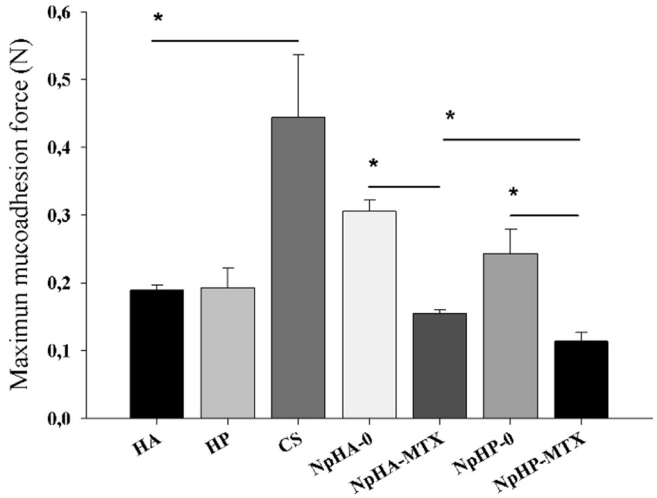

Fig. 3. Maximum mucoadhesion force (N) between intestine mucosa and polymers, empty or loaded nano PECs. Results are expressed as mean (n = 3) and bars represent the SD.The signal (*) denotes a significant difference ($p < 0.05$).

(Fig. 3), where the NpHA-MTX and NpHP-MTX samples presented lower Fm, compared to NpHA-0 and NpHP-0 ($p < 0.05$). Due to the positive ZP of the particles and the anionic characteristic of the mucin, presented in the mucus, the electrostatic interaction should be the main force responsible for the consolidation of the mucoadhesion process.

The MTX addition promoted a significant reduction of the positive residual charge of the nano PECs (Table 2) which consequently reduces the attraction and interaction force between the surface of the system and the biological substrate. NpHA-MTX showed even higher Fm compared to NpHP-MTX ($p < 0.05$). The higher %AE of NpHP-MTX contributed to the reduction of it positive ZP and, according to the particle size analysis, may had led to the formation of additional points of electrostatic interaction between the ionizable groups of the polymers, rearranging the polymer chains, forming a more packed polymer network, responsible for the reduction of it average diameter. Considering that in the NpHA-MTX the mesh is more dilated (higher average diameter) compared to the NpHP-MTX, the swelling process should be facilitated and a greater flexibility of the chains should be achieved, favouring the interaction with the glycoprotein chains present in the mucus and the consolidation of the adhesion process (Andrews et al., 2009; Smart, 2005).

3.4. Cell viability studies

In order to evaluate the biocompatibility and safety of the nano PECs for the oral administration and intestine site of action, the *in vitro* cell viability studies were carried out with Caco-2 and HT29-MTX intestinal cells. Samples and controls were incubated with cells, for 4 and 24 h, and cell viability was assessed by MTT assay. The cytotoxicity of the polymeric constituents of the nano PECs was initially evaluated (Fig. 4).

It is possible to observe that even after 24 h of incubation with the polymers, the percentage of Caco-2 and HT29-MTX cell lines viability was higher than 70%, for all tested concentrations. For HA and HP an increasing in cell viability was observed after 24 h, that not occurs to CS due this polymer could slightly perturbed the cells plasma membrane, in a reversible or irreversible way (Thanou et al., 2001). However, the results evidenced that CS, HA and HP were safe excipients to nano PECs formulations. Empty and loaded nano PECs cytotoxicity as a drug carrier to the small intestine were evaluated and compared to the free MTX. The results are shown in Fig. 5.

For Caco-2 cell viability after 4 h of incubation, no relevant difference was observed between samples and the free drug. After incubation by 24 h, it was noticed a slight decrease in the Caco-2 cell viability, that was more pronounced for NpHA-MTX and NpHP-MTX at concentrations 10 μg/mL (57% and 45%, respectively) and 100 μg/mL (51% and 40%, respectively), indicating that in these higher concentration a maximization of CS and MTX cytotoxicity effect may occurred. HT29-MTX cell line, shown higher viability, when in contact with all tested samples (> 80% in 4 h and > 60% in 24 h), compared to Caco-2 cell line (Fig. 5). These higher values of viability could be explained by the production and secretion of a mucus layer; which represents a physic barrier, protecting the cells (Antunes et al., 2013; Shrestha et al., 2016). In brief, besides evaluated the system safety, these studies were used to choose the nontoxic and measurable concentration to perform the *in vitro* permeability studies.

3.5. In vitro intestinal permeability studies

In addition to the physical-chemical characterization, it was extremely important the evaluation of biological performance of the nano PECs by a cellular model that mimics the physiological conditions of the gastrointestinal system. *In vitro* methods using cell culture presents several advantages compared to the *in vivo* ones, such as reduction of the number of experimental variables, more reproducible data, less time of execution besides the low cost. The Caco-2 cell line is one of the

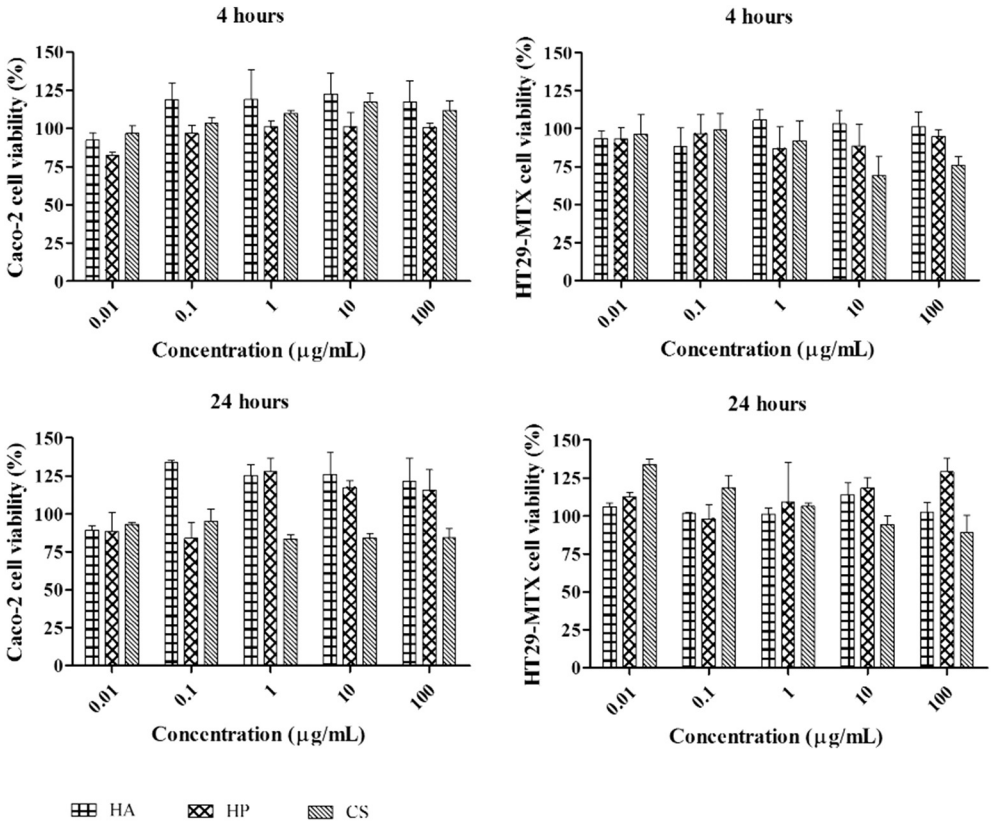

Fig. 4. Cell viability (%) of Caco-2 and HT29-MTX cell lines after 4 h and 24 h of incubation with increasing concentrations of polymers (mean ± SD).

most used in this studies because its functional and structural behaviour similar to the enterocytes; which comprise the epithelium of the small intestine, with the expression of important surface transporters such as P-gp, that act to reduce the intestinal permeability of drugs as MTX. However, Caco-2 monocultures are not able to mimic the complex structure and interactions between cellular elements, such as tight junction, as well as to produce the mucus layer that form the protective barrier of the mucosa (Araujo and Sarmento, 2013; Leonard et al.,

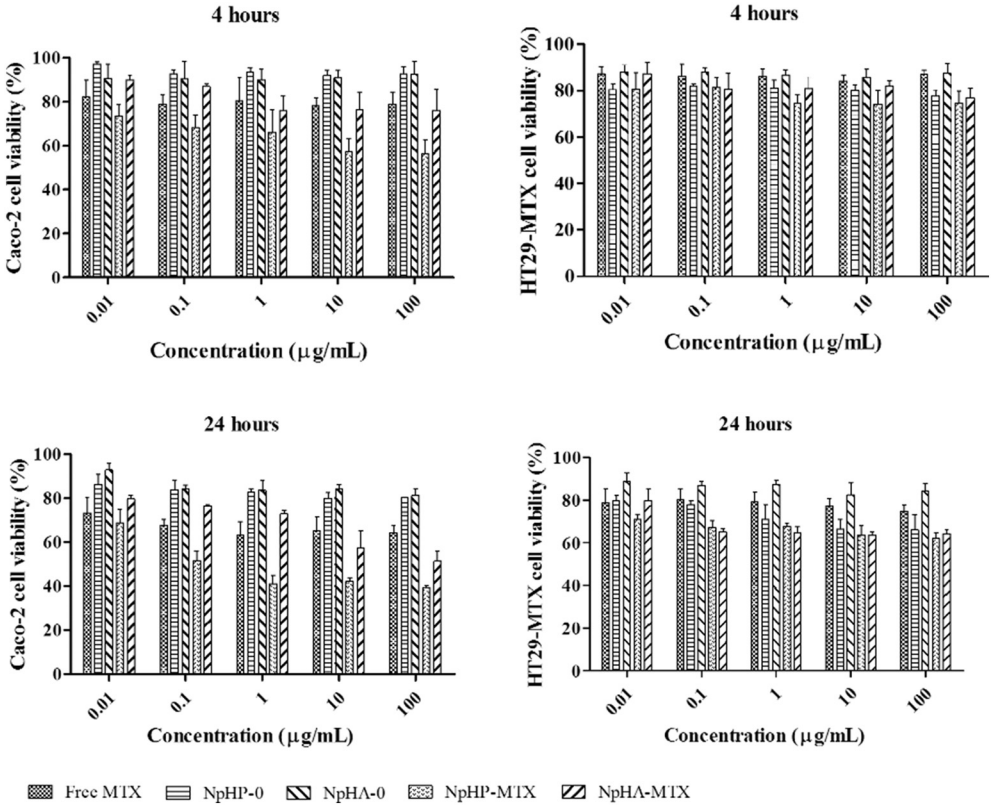

Fig. 5. Cell viability (%) of Caco-2 and HT29-MTX cell lines after 4 h and 24 h of incubation with increasing concentrations of free MTX, empty and loaded nano PECs (mean ± SD).

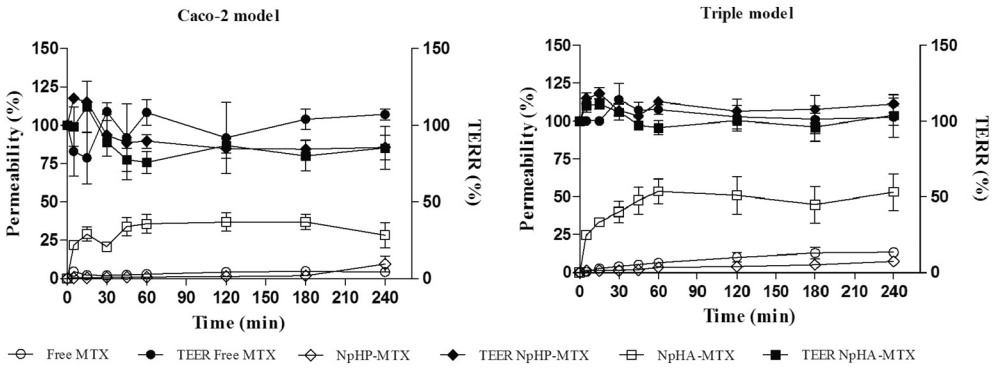

Fig. 6. Permeability profile of free MTX, MTX from NpHP-MTX and NpHA-MTX, across the Caco-2 monoculture and triple models and TEER measurements of the cell monolayers as a function of time during the permeability tests. Results are expressed as mean (n = 3) ± SD.

2010; Shah et al., 2006). Thus, differently of the monoculture, the triple co-culture model is a more complex model, consisted by Caco-2 cells, HT29-MTX; cells capable of secreting mucus and Raji B cells lymphocytes; which induce the differentiation of Caco-2 cells into M cells (Antunes et al., 2013; Araujo and Sarmento, 2013). In order to evaluate the impact of the systems properties in the MTX permeability and in the cellular interaction, as well as the mucus effect on these biological properties, the Caco-2 mono-culture and triple co-culture, consolidated models for this study, were used. Based on viability studies, the non-toxic concentration of 100 μg/mL of free MTX, NpHA-MTX and NpHP-MTX (related to the drug concentration) was selected. The samples permeability profile is shown in Fig. 6.

All the 21 days of cells cultivation, the TEER values of both models were monitored to ensure the monolayer formation. During and after the experiment these values were kept around 100% proving the integrity of the Caco-2 monolayer and triple model.

As it is possible to observe in Fig. 6, the permeability profile of free MTX and NpHP-MTX were similar, for both cell models; Caco-2 monolayer and triple model during 240 min. Concerning the NpHA-MTX, a different profile was observed, with higher drug permeation. For Caco-2 model, after 240 min, 28.3% of the MTX crossed the monolayer, almost 3 times more than the free drug and NpHP-MTX. In the triple co-culture cell model, the permeability of MTX loaded in NpHA-MTX increased faster, achieving 5 times more permeated drug compared to the free drug and 2-fold increase compared to NpHA-MTX permeated percentage across the Caco-2 monoculture. This behaviour can be attributed to the higher mucoadhesiveness of the NpHA-MTX (Section 3.3); which allows to the stronger interaction of this system with the mucus layer produced by the HT29-MTX cells, inducing, consequently, an increase in the local drug gradient and in the permeability. In addition, we can suggest that in NpHA-MTX, the cationic sites of CS were more available, observed by the higher positive ZP (Table 2), compared to the NpHP-MTX. As known, mainly by electronic interaction, CS has an effect in open reversibly the cells junctions (Rinaudo, 2011; Yeh et al., 2011).

The drug apparent permeability (Papp), percentage of MTX in the apical side (%AS) and accumulated in the cells (%CE) are shown in Table 3.

The highest Papp values for sample NpHA-MTX corroborate the behaviour observed in Fig. 6, so that Papp values for NpHA-MTX were approximately 3-fold and 7.5-fold higher than the NpHP-MTX in the monoculture and triple co-culture cell models, respectively, although the %CE values for both systems were similar in the monoculture (approximately 10%), indicating a similar biological interaction. On the other hand, in the triple co-culture the %CE for NpHA-MTX was slightly higher than that of NpHP-MTX, which may be related to the higher mucoadhesive capacity of this system. The enhancement of MTX permeation may be a favourable feature in the design of oral systems in which a systemic effect of the drug is desired. Despite NpHP-MTX showed a similar permeability profile to that of free MTX (Fig. 6), a higher percentage of drug accumulated in the cells (%CE) was observed (Table 3), compared to free MTX (10–10.9% for NpHP-MTX and 4.1–4.7% for MTX), in the monoculture and triple co-culture cell models. The lower Papp of the free MTX and the high percentage of drug in the apical side (%AS) in the end of the assay supports that MTX is a P-gp substrate with low permeability and cell accumulation. The modulation of the biological interaction, mainly the improvement of %CE associated to the low permeability, reveals the potential of the NpHP-MTX use in the local treatment of pathologies such as inflammatory bowel diseases and colonic tumours.

3.5.1. *Confocal laser scanning microscopy*

After permeability studies, the integrity of the monolayer in monoculture and triple models was analysed with confocal microscopy. A confluent monolayer with the presence of tight-junctions was found for all samples. Even for the NpHA-MTX, that showing a very high permeability of MTX the image shows that the Caco-2 monoculture and triple models were confluent (Fig. 7). According to the MTT assays, NpHP-MTX and NpHA-MTX did not induce any sign of toxicity and therefore, cannot explain difference in terms of permeability. Moreover, it is possible to observe a lower expression of tight-junctions in the triple model, which is consistent to the presence of goblet and M cells.

4. Conclusions

Innovative nano PECs of chitosan/hyaluronic acid containing or not hypromellose phthalate were successfully obtained by polyelectrolyte complexation technic, avoiding organic solvents and high energy conditions. Methotrexate, a high solubility and low permeability drug, was loaded in the nano PECs. The mucoadhesiveness of all samples was demonstrated by an *ex vivo* assay and the influence of the polymers and drug in this property was discussed in detail. Nano PECs were evaluated

Table 3
Samples Papp, MTX apical side percentage (%AS) and MTX bound to or within the cells (%CE). Results are expressed in mean ± SD.

Sample	Caco-2 monoculture			Triple co-culture model		
	Papp × 10^6 (cm/s)	% AS	%CE	Papp × 10^6 (cm/s)	% AS	%CE
Free MTX	1.0 ± 0.2	75.4 ± 7.9	4.7 ± 0.5	3.0 ± 0.05	83.0 ± 9.7	4.1 ± 1
NpHP-MTX	2.1 ± 1.1	61.3 ± 1.7	10.0 ± 1.9	1.6 ± 0.4	60.4 ± 2.5	10 ± 0.4
NpHA-MTX	6.3 ± 1.8	31.4 ± 13.4	10.8 ± 0.9	11.8 ± 2.7	27.8 ± 9.1	18.1 ± 6

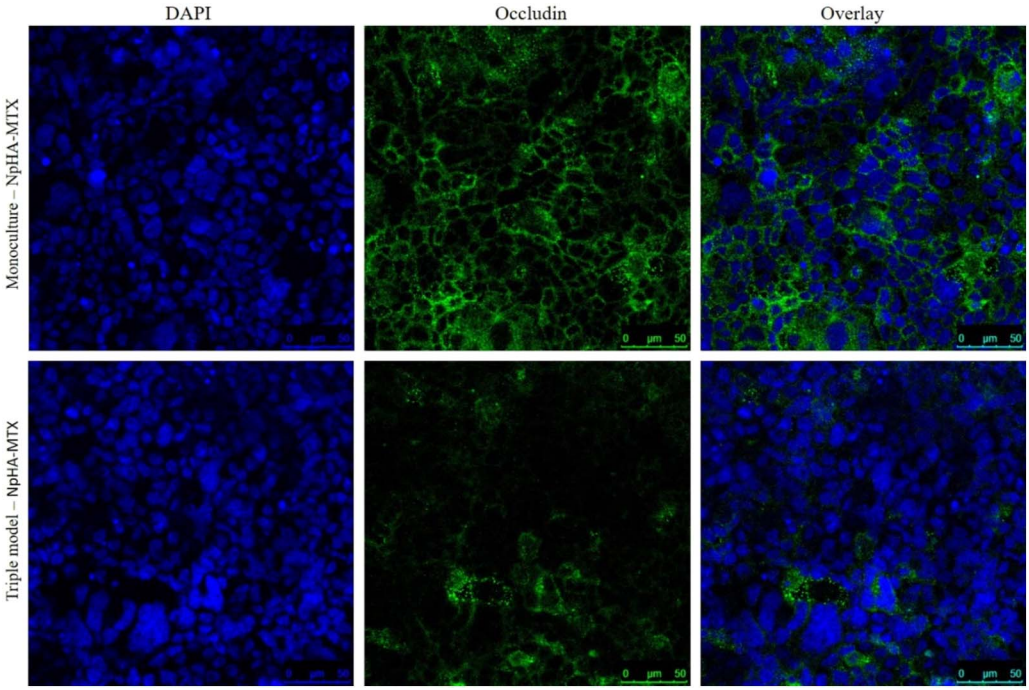

Fig. 7. Immunofluorescence showing the morphology of the monoculture and the triple model after permeability of NpHA-MTX. Occludin tight-junctions were labelled in green and nucleus was counter-stained with DAPI in blue. Images were obtained at a high magnification (× 63 in immersion oil). (For interpretation of the references to colour in this figure legend, the reader is referred to the web version of this article.)

regarding their cytotoxicity in Caco-2 and HT29-MTX cell lines and *in vitro* permeability across monoculture and triple co-culture cell models. The cell viability studies showed the safety of the pristine polymers and nano PECs for oral administration, in a range of concentration of 0.01 to 100 µg/mL. The loading of MTX in the nano PECs allowed a significant increasing in the cellular accumulation, compared to the free MTX, evidencing the changing of biological interaction pattern of the developed nanocarriers. NpHA-MTX allowed a high MTX permeability, across a Caco-2 monoculture and a triple co-culture cell model; in which the mucus produced by HT29-MTX cells did not represented an obstacle, despite the higher mucoadhesiveness of this sample. The results indicating that the NPHA-MTX sample was able to improve the drug intestinal permeability, a promising result to the systemic action of MTX. In contrast, with NpHP-MTX, a reduction of MTX permeability across both cell models was observed, with higher percentage of cellular accumulation in both cell models, compared to the free MTX. This biological interaction pattern is a favorable feature when local action of MTX is desired as for the local treatment of diseases as intestinal bowel disease and/or colorectal cancer. In such way, with a simple modification in the nano PECs matrix compounding, by adding hypromellose phthalate, a modulation of MTX permeability behavior can be achieved.

Conflict of interest

The authors declare that they have no conflict of interest.

Acknowledgments

The authors are thankful to FAPESP (Fundação de Amparo à Pesquisa do Estado de São Paulo), Capes and to São Paulo State University (Unesp), School of Pharmaceutical Sciences, Araraquara, for providing financial and structural support to develop this work. Anna Lechanteur would like to acknowledge the Fonds Leon Fredericq for financial support. Andreia Almeida would like to thank Fundação para a Ciência e a Tecnologia (FCT), Portugal, for the financial support. This article is a result of the project NORTE-01-0145-FEDER-000012, supported by Norte Portugal Regional Operational Programme (NORTE 2020), under the PORTUGAL 2020 Partnership Agreement, through the European Regional Development Fund (ERDF).

This work was financed by FEDER - Fundo Europeu de Desenvolvimento Regional funds through the COMPETE 2020 - Operacional Programme for Competitiveness and Internationalisation (POCI), Portugal 2020, and by Portuguese funds through FCT - Fundação para a Ciência e a Tecnologia/Ministério da Ciência, Tecnologia e Ensino Superior in the framework of the project “Institute for Research and Innovation in Health Sciences” (POCI-01-0145-FEDER-007274).

References

Abolmaali, S.S., Tamaddon, A.M., Dinarvand, R., 2013. A review of therapeutic challenges and achievements of methotrexate delivery systems for treatment of cancer and rheumatoid arthritis. Cancer Chemother. Pharmacol. 71, 1115–1130.

Almeida, A., Silva, D., Gonçalves, V., Sarmento, B., 2017. Synthesis and characterization of chitosan-grafted-polycaprolactone micelles for modulate intestinal paclitaxel delivery. Drug Deliv. Transl. Res. 1–11.

Andrews, G.P., Laverty, T.P., Jones, D.S., 2009. Mucoadhesive polymeric platforms for controlled drug delivery. Eur. J. Pharm. Biopharm. 71, 505–518.

Antunes, F., Andrade, F., Araujo, F., Ferreira, D., Sarmento, B., 2013. Establishment of a triple co-culture in vitro cell models to study intestinal absorption of peptide drugs. Eur. J. Pharm. Biopharm. 83, 427–435.

Araujo, F., Sarmento, B., 2013. Towards the characterization of an in vitro triple co-culture intestine cell model for permeability studies. Int. J. Pharm. 458, 128–134.

Asane, G.S., Nirmal, S.A., Rasal, K.B., Naik, A.A., Mahadik, M.S., Rao, Y.M., 2008. Polymers for mucoadhesive drug delivery system: a current status. Drug Dev. Ind. Pharm. 34, 1246–1266.

Barrueco, J.R., O'Leary, D.F., Sirotnak, F.M., 1992. Metabolic turnover of methotrexate polyglutamates in lysosomes derived from S180 cells. Definition of a two-step process limited by mediated lysosomal permeation of polyglutamates and activating reduced sulfhydryl compounds. J. Biol. Chem. 267, 15356–15361.

Becker, L.C., Bergfeld, W.F., Belsito, D.V., Klaassen, C.D., Marks, J.G., Shank, R.C., Slaga, T.J., Snyder, P.W., Andersen, F.A., 2009. Final report of the safety assessment of hyaluronic acid, potassium hyaluronate, and sodium hyaluronate. Int. J. Toxicol. 28, 5–67.

Boni, F.I., Prezotti, F.G., Cury, B.S., 2016. Gellan gum microspheres crosslinked with trivalent ion: effect of polymer and crosslinker concentrations on drug release and mucoadhesive properties. Drug Dev. Ind. Pharm. 42, 1283–1290.

Borst, P., Evers, R., Kool, M., Wijnholds, J., 1999. The multidrug resistance protein family. Biochim. Biophys. Acta 1461, 347–357.

Carvalho, F.C., Bruschi, M.L., Evangelista, R.C., Gremião, M.P.D., 2010. Mucoadhesive drug delivery systems. Braz. J. Pharm. Sci. 46, 1–17.

Carvalho, F.C., Calixto, G., Hatakeyama, I.N., Luz, G.M., Gremião, M.P., Chorilli, M., 2013. Rheological, mechanical and bioadhesive behavior of hydrogels to optimize skin delivery systems. Drug Dev. Ind. Pharm. 39, 1750–1757.

Cascone, M.G., Lazzeri, L., Carmignani, C., Zhu, Z., 2002. Gelatin nanoparticles produced

by a simple W/O emulsion as delivery system for methotrexate. J. Mater. Sci. Mater. Med. 13, 523–526.
Chadha, R., Arora, P., Kaur, R., Saini, A., Singla, M., Jain, D., 2009. Characterization of solvatomorphs of methotrexate using thermoanalytical and other techniques. Acta Pharma. 59, 245–257.
Chae, S.Y., Jang, M.K., Nah, J.W., 2005. Influence of molecular weight on oral absorption of water soluble chitosans. J. Control. Release 102, 383–394.
Ensign, L.M., Schneider, C., Suk, J.S., Cone, R., Hanes, J., 2012. Mucus penetrating nanoparticles: biophysical tool and method of drug and gene delivery. Adv. Mater. 24, 3887–3894.
Ferreira, N.N., Perez, T.A., Pedreiro, L.N., Prezotti, F.G., Boni, F.I., Cardoso, V.M.D.O., Venâncio, T., Gremião, M.P.D., 2017. A novel pH-responsive hydrogel based on calcium alginate engineered by the previous formation of polyelectrolyte complexes (PECs) intended to vaginal administration. Drug Dev. Ind. Pharm. 1–33.
Fukasawa, M., Obara, S., 2003. Molecular weight determination of hypromellose phthalate (HPMCP) using size exclusion chromatography with a multi-angle laser light scattering detector. Chem. Pharm. Bull. (Tokyo) 51, 1304–1306.
Gaies, E., Jebabli, N., Trabelsi, S., Salouage, I., Charfi, R., Lakhal, M., Klouz, A., 2012. Methotrexate side effects: review article. J. Drug. Metab. Toxicol. 3, 1–5.
Gamboa, J.M., Leong, K.W., 2013. In vitro and in vivo models for the study of oral delivery of nanoparticles. Adv. Drug Deliv. Rev. 65, 800–810.
Gao, H., Yang, W., Min, K., Zha, L., Wang, C., Fu, S., 2005. Thermosensitive poly(*N*-isopropylacrylamide) nanocapsules with controlled permeability. Polymer 46, 1087–1093.
Gaumet, M., Vargas, A., Gurny, R., Delie, F., 2008. Nanoparticles for drug delivery: the need for precision in reporting particle size parameters. Eur. J. Pharm. Biopharm. 69, 1–9.
Gorlick, R., Goker, E., Trippett, T., Steinherz, P., Elisseyeff, Y., Mazumdar, M., Flintoff, W.F., Bertino, J.R., 1997. Defective transport is a common mechanism of acquired methotrexate resistance in acute lymphocytic leukemia and is associated with decreased reduced folate carrier expression. Blood 89, 1013–1018.
Hamidi, M., Azadi, A., Rafiei, P., 2008. Hydrogel nanoparticles in drug delivery. Adv. Drug Deliv. Rev. 60, 1638–1649.
Haxaire, K., Maréchal, Y., Milas, M., Rinaudo, M., 2003. Hydration of polysaccharide hyaluronan observed by IR spectrometry. I. preliminary experiments and band assignments. Biopolymers 72, 10–20.
Higano, C.S., Livingston, R.B., 1989. Oral dipyridamole and methotrexate in human solid tumors: a toxicity trial. Cancer Chemother. Pharmacol. 23, 259–262.
Hokputsaa, S., Jumel, K., Alexander, C., Harding, S.E., 2003. Hydrodynamic characterisation of chemically degraded hyaluronic acid. Carbohydr. Polym. 52, 111–117.
Huber, P.C., Maruiama, C.H., Almeida, W.P., 2010. P-glycoprotein and multidrug resistance: structure-activity relationships of modulators. Quim Nova 33, 2148–2154.
Jachens, A.W., Chu, D.S., 2008. Retrospective review of methotrexate therapy in the treatment of chronic, noninfectious, nonnecrotizing scleritis. Am J. Ophthalmol. 145, 487–492.
Jain, R.K., Wei, J., Gullino, P.M., 1979. Pharmacokinetics of methotrexate in solid tumors. J. Pharmacokinet. Biopharm. 7, 181–194.
Janes, K.A., Calvo, P., Alonso, M.J., 2001. Polysaccharide colloidal particles as delivery systems for macromolecules. Adv. Drug Deliv. Rev. 47, 83–97.
Leonard, F., Collnot, E.M., Lehr, C.M., 2010. A three-dimensional coculture of enterocytes, monocytes and dendritic cells to model inflamed intestinal mucosa in vitro. Mol. Pharm. 7, 2103–2119.
Li, C., Hein, S., Wang, K., 2013. Chitosan-carrageenan polyelectrolyte complex for the delivery of protein drugs. ISRN Biomaterials 2013, 1–6.
Liao, Y.-H., Jones, S.A., Forbes, B., Martin, G.P., Brown, M.B., 2005. Hyaluronan: pharmaceutical characterization and drug delivery. Drug Deliv. 12, 327–342.
Madsen, F., Eberth, K., Smart, J.D., 1998. A rheological examination of the mucoadhesive/mucus interaction: the effect of mucoadhesive type and concentration. J. Control. Release 50, 167–178.
Makhlof, A., Tozuka, Y., Takeuchi, H., 2011. Design and evaluation of novel pH-sensitive chitosan nanoparticles for oral insulin delivery. Eur. J. Pharm. Sci. 42, 445–451.
Martins, S.J., Yamamoto, C.A., 2008. Clinical and economic issues in adjuvant chemotherapy for HER-2 positive breast cancer. Rev. Assoc. Med. Bras. 54, 494–499.
Meehan, E., 2006. Characterisation of hydroxypropylmethylcellulose phthalate (HPMCP) by GPC using a modified organic solvent. Anal. Chim. Acta 557, 2–6.
Meera, G.T., Abraham, E., 2006. Polyionic hydrocolloids for the intestinal delivery of protein drugs: alginate and chitosan — a review. J. Control. Release 114, 1–14.
Mizrahy, S., Raz, S.R., Hasgaard, M., Liu, H., Soffer-Tsur, N., Cohen, K., Dvash, R., Landsman-Milo, D., Bremer, M.G.E.G., Moghimi, S.M., Peer, D., 2011. Hyaluronan-coated nanoparticles: the influence of the molecular weight on CD44-hyaluronan interactions and on the immune response. J. Control. Release 156, 231–238.
Murphy, R.M., 1997. Static and dynamic light scattering of biological macromolecules: what can we learn? Curr. Opin. Biotechnol. 8, 25–30.
Pedreiro, L.N., Stringhetti, B., Cury, F., Gremião, M.P., 2016. Mucoadhesive nanostructured polyelectrolyte complexes as potential carrier to improve zidovudine permeability. J. Nanosci. Nanotechnol. 16, 1248–1256.
Ponta, H., Sherman, L., Herrlich, P.A., 2003. CD44: From adhesion molecules to signalling regulators. Nat. Rev. Mol. Cell Biol. 4, 33–45.
Reddy, K.J., Karunakaran, K.T., 2013. Purification and characterization of hyaluronic acid produced by Streptococcus zooepidemicus strain 3523-7. J. BioSci. Biotech. 2, 173–179.
Rinaudo, M., 2011. Chitin and chitosan: properties and applications. Prog. Polym. Sci. 31, 603–632.
Sarmento, B., Ribeiro, A., Veiga, F., Sampaio, P., Neufeld, R., Ferreira, D., 2007. Alginate/chitosan nanoparticles are effective for oral insulin delivery. Pharm. Res. 24, 2198–2206.
Schatz, C., Pichot, C., Delair, T., Viton, C.D., 2003. Static lights studies on chitosan solutions: from macromolecular chains to colloidal dispersions. Langmuir 19, 9896–9903.
Schatz, C., Domard, A., Viton, C., Pichot, C., Delair, T., 2004. Versatile and efficient formation of colloids of biopolymer-based polyelectrolyte complexes. Biomacromolecules 5, 1882–1892.
Shah, P., Jogani, V., Bagchi, T., Misra, A., 2006. Role of Caco-2 cell monolayers in prediction of intestinal drug absorption. Biotechnol. Prog. 22, 186–198.
Shrestha, N., Araújo, F., Shahbazi, M.-A., Mäkilä, E., Gomes, M.J., Herranz-Blanco, B., Lindgren, R., Granroth, S., Kukk, E., Salonen, J., Hirvonen, J., Sarmento, B., Santos, H.A., 2016. Thiolation and cell-penetrating peptide surface functionalization of porous silicon nanoparticles for oral delivery of insulin. Adv. Funct. Mater. 26, 3405–3416.
Silva, D.S., Almeida, A., Prezotti, F., Cury, B., Campana-Filho, S.P., Sarmento, B., 2017. Synthesis and characterization of 3,6-*O*,*O*′-dimyristoyl chitosan micelles for oral delivery of paclitaxel. Colloid. Surface. B. 152, 220–228.
Smart, J.D., 2005. The basics and underlying mechanisms of mucoadhesion. Adv. Drug Deliv. Rev. 57, 1556–1568.
Sosnik, A., Das Neves, J., Sarmento, B., 2014. Mucoadhesive polymers in the design of nano-drug delivery systems for administration by non-parenteral routes: a review. Prog. Polym. Sci. 39, 2030–2075.
Thanou, M., Verhoef, J., Junginger, H., 2001. Oral drug absorption enhancement by chitosan and its derivatives. Adv. Drug Deliv. Rev. 52, 117–126.
Thiebaut, F., Tsuruo, T., Hamada, H., Gottesman, M.M., Pastan, I., Willingham, M.C., 1987. Cellular localization of the multidrug-resistance gene product P-glycoprotein in normal human tissues. Proc. Natl. Acad. Sci. U. S. A. 84, 7735–7738.
Trapani, A., Denora, N., Iacobellis, G., Sitterberg, J., Bakowsky, U., Kissel, T., 2011. Methotrexate-loaded chitosan- and glycol chitosan-based nanoparticles: a promising strategy for the administration of the anticancer drug to brain tumors. AAPS PharmSciTech 12, 1302–1311.
Valente, J.J., Payne, R.W., Manning, M.C., Wilson, W.W., Henry, C.S., 2005. Colloidal behavior of proteins: effects of the second virial coefficient on solubility, crystallization and aggregation of proteins in aqueous solution. Curr. Pharm. Biotechnol. 6, 427–436.
Varum, F.O., Basit, A.W., Sousa, J., Veiga, F., 2008. Mucoadhesion studies in the gastrointestinal tract to increase oral drug bioavailability. Braz. J. Pharm. Sci. 44, 535–547.
Varum, F.J., Veiga, F., Sousa, J.S., Basit, A.W., 2010. An investigation into the role of mucus thickness on mucoadhesion in the gastrointestinal tract of pig. Eur. J. Pharm. Sci. 40, 335–341.
Vllasaliu, D., Exposito-Harris, R., Heras, A., Casettari, L., Garnett, M., Illum, L., Stolnik, S., 2010. Tight junction modulation by chitosan nanoparticles: comparison with chitosan solution. Int. J. Pharm. 400, 183–193.
Wang, X.Q., Dai, J.D., Chen, Z., Zhang, T., Xia, G.M., Nagai, T., Zhang, Q., 2004. Bioavailability and pharmacokinetics of cyclosporine A-loaded pH-sensitive nanoparticles for oral administration. J. Control. Release 97, 421–429.
Wang, A.Z., Langer, R., Farokhzad, O.C., 2012. Nanoparticle delivery of cancer drugs. Annu. Rev. Med. 63, 185–198.
Wang, J., Kong, M., Zhou, Z., Yan, D., Yu, X., Cheng, X., Feng, C., Liu, Y., Chen, X., 2017. Mechanism of surface charge triggered intestinal epithelial tight junction opening upon chitosan nanoparticles for insulin oral delivery. Carbohydr. Polym. 157, 596–602.
Widemann, B.C., Adamson, P.C., 2006. Understanding and managing methotrexate nephrotoxicity. Oncologist 11, 694–703.
Yang, Y., Wang, S., Wang, Y., Wang, X., Wang, Q., Chen, M., 2014. Advances in self-assembled chitosan nanomaterials for drug delivery. Biotechnol. Adv. 32, 1301–1316.
Yeh, T.-H., Hsu, L.-W., Tseng, M.T., Lee, P.-L., Sonjae, K., Ho, Y.-C., Sung, H.-W., 2011. Mechanism and consequence of chitosan-mediated reversible epithelial tight junction opening. Biomaterials 32, 6164–6173.
Zhang, X., Sun, M., Zheng, A., Cao, D., Bi, Y., Sun, J., 2012. Preparation and characterization of insulin-loaded bioadhesive PLGA nanoparticles for oral administration. Eur. J. Pharm. Sci. 45, 632–638.